

Supporting Information for

Characterization of Hedgehog Acyltransferase Inhibitors Identifies a Small Molecule Probe for Hedgehog Signaling by Cancer Cells

Ursula R. Rodgers^{a,1}, Thomas Lanyon-Hogg^b, Naoko Masumoto^{b,2}, Markus Ritzefeld^b, Rosemary Burke^c, Julian Blagg^c, Anthony I. Magee^{a,*}, Edward W. Tate^{b,*}

^a Molecular Medicine Section, National Heart & Lung Institute, Imperial College London, SW7 2AZ, UK. Tel: +44 (0)20 7594 3135. E-mail: t.magee@imperial.ac.uk

^b Department of Chemistry, Imperial College London, SW7 2AZ, UK; Tel: +44 (0)20 7594 3752. E-mail: e.tate@imperial.ac.uk

^c Cancer Research UK Cancer Therapeutics Unit, The Institute of Cancer Research, London, SW7 3RP, UK

¹ Current address: Electron Microscopy Unit, Royal Brompton Hospital, The Institute of Cancer Research, London, SW3 6NP, UK

² Current address: Imanova Limited, Hammersmith Hospital, London, W12 0NN, UK

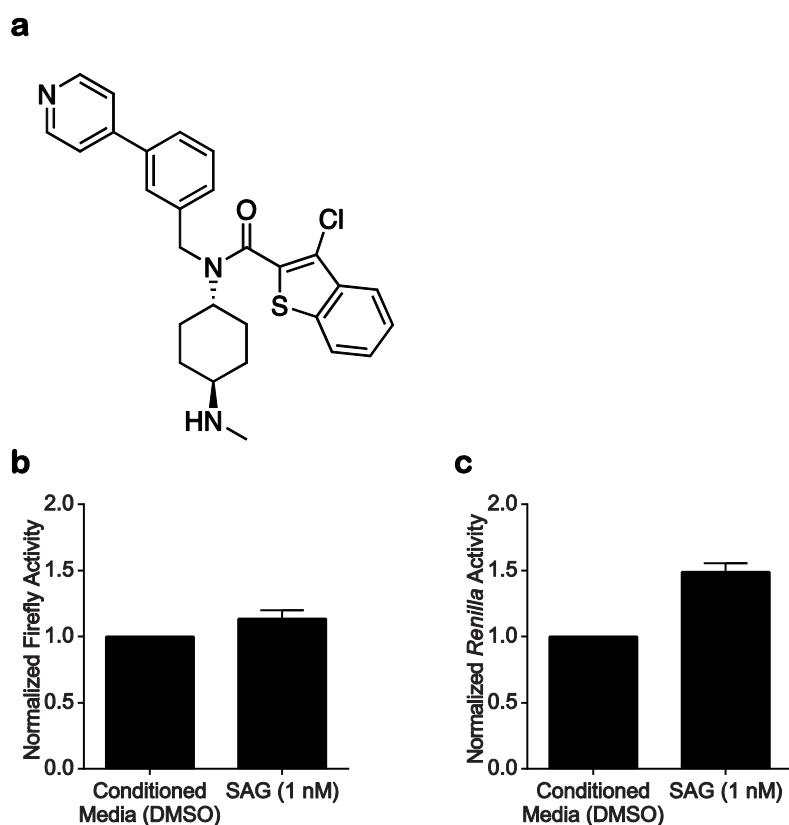
* Corresponding authors

TABLE OF CONTENTS

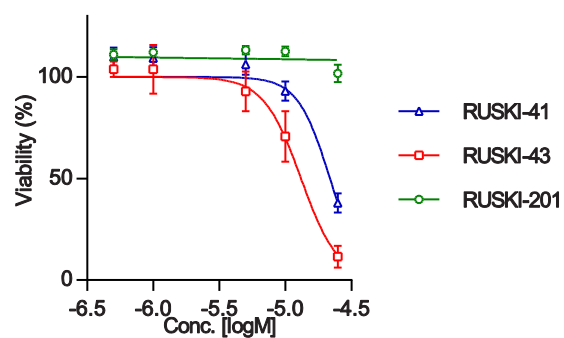
TABLE OF CONTENTS	2
SUPPLEMENTARY FIGURES	4
Supplementary Figure S1. Comparison of vehicle-treated conditioned media and Smoothened agonist (SAG).	4
Supplementary Figure S2. Effect of RUSKI inhibitors on viability of Shh-Light2 cells.	5
Supplementary Figure S3. Effect of RUSKI inhibitors on <i>Renilla</i> luciferase activity.	6
Supplementary Figure S4. Effect of RUSKI-43, RUSKI-201 and LGK974 on Wnt signaling.	7
Supplementary Figure S5. Structure of bioorthogonal capture reagents.	8
Supplementary Figure S6. Chemoproteomic profiling of the effect of RUSKI-41 treatment on protein palmitoylation.	9
Supplementary Figure S7. Expression of HHAT and SHH in pancreatic, lung and breast tumor cell lines.	10
Supplementary Figure S8. Effect of Smo inhibitor GDC-0449 on Hh signaling induced by tumor cell lines.	11
Supplementary Figure S9. Effect of GDC-0449, RUSKI-43, and RUSKI-201 on the viability of Panc-1 and MCF-7 cells.	12
Supplementary Figure S10. Effect of RUSKI-201 on <i>Renilla</i> luciferase activity of Shh-Light2 cells co-cultured with cancer cell lines.	13
Supplementary Figure S11. Effect of RUSKI-201 and GDC-0449 on cell viability.	14
SUPPLEMENTARY TABLES.....	15
Supplementary Table S1. Palmitoylated proteins identified by YnPal-tagging in response to RUSKI-201 treatment using spike-in SILAC-based quantitative proteomics.....	15
Supplementary Table S2. Palmitoylated proteins identified by YnPal-tagging in response to RUSKI-41 treatment using spike-in SILAC-based quantitative proteomics.....	18
MATERIALS AND METHODS	19
Reagents	19
Chemical Synthesis	19
Cell Lines and Tissue Culture Reagents	19
Shh-Light2 Assay	19
Inhibition of media conditioning by RUSKI compounds	19
Off-target effects of RUSKI compounds on Shh-Light2 cells.....	20
Recovery of canonical Hh signaling by SAG	20
Co-culture of cancer cell lines	20
Wnt signaling assay.....	20
Cell viability assay	21
CyQUANT direct cell proliferation assay.....	21

CellTiter-Glo viability assay	21
<i>In vitro</i> palmitoylation, bioorthogonal ligation and western blotting	21
Proteomics.....	22
RNA Isolation and quantitative real-time PCR	23
Software and data analysis	23
REFERENCES.....	24

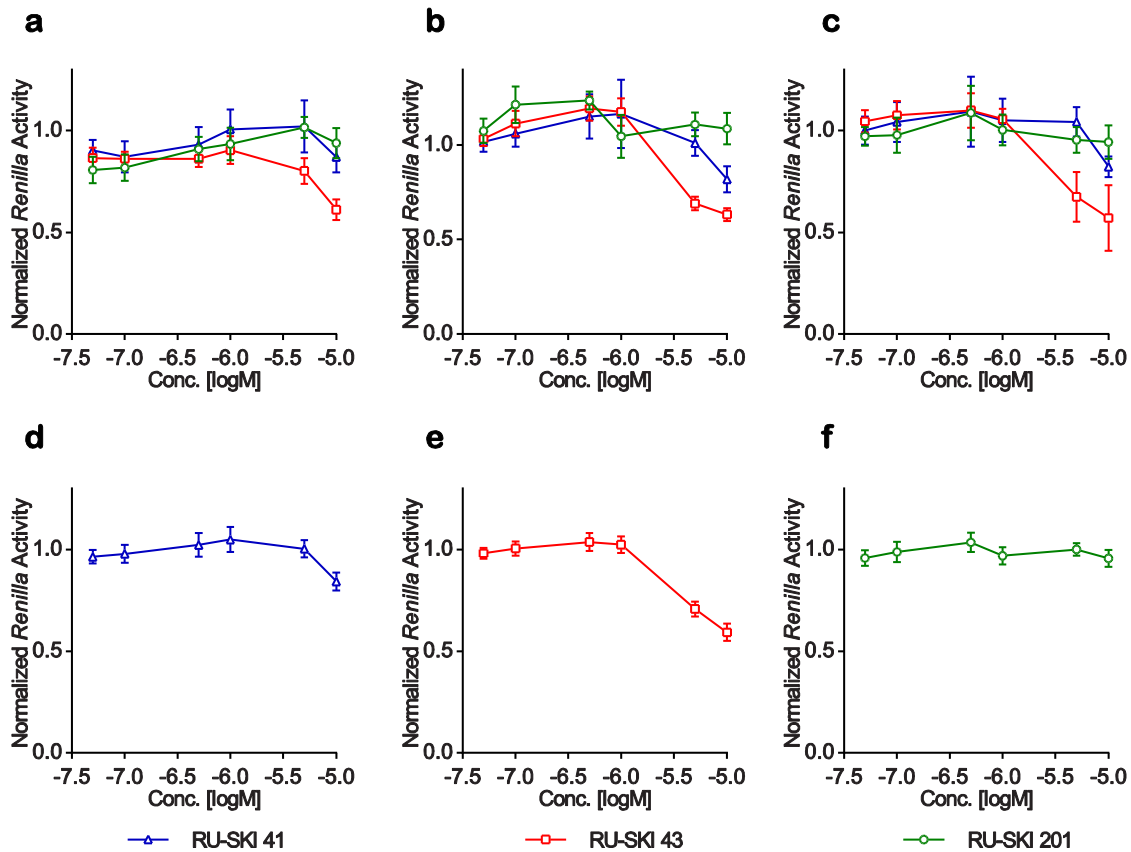
SUPPLEMENTARY FIGURES



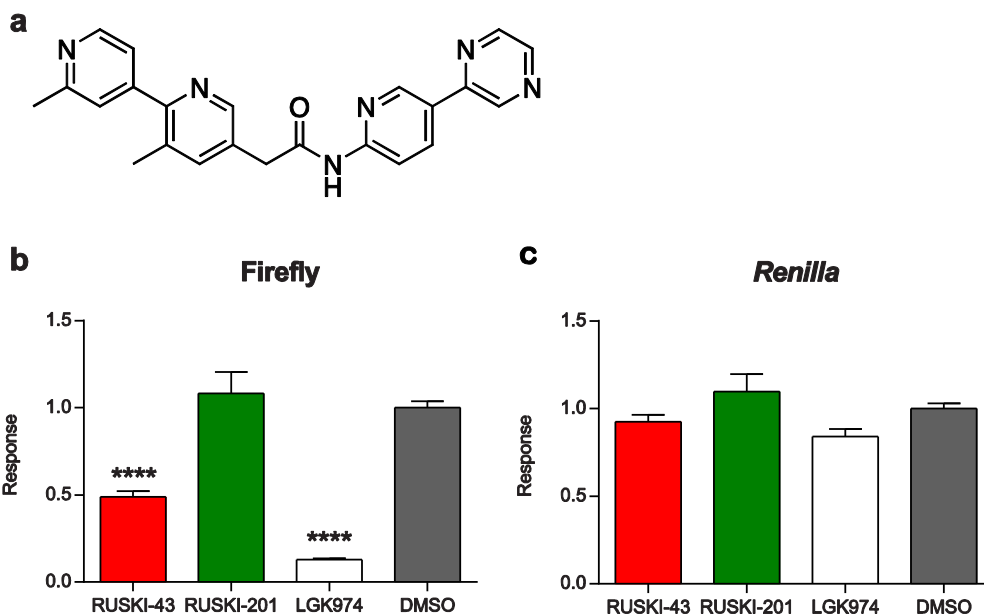
Supplementary Figure S1. Comparison of vehicle-treated conditioned media and Smoothed agonist (SAG). (a) Structure of SAG.¹ (b) The effect of SAG alone was compared to HEK-293 Shh⁺ medium conditioned in the presence of DMSO vehicle. After 48 h incubation of media with Shh-Light2 cells, the cells were lysed and the activities of firefly and (c) *Renilla* luciferases were measured. Response was normalized to vehicle-only control. Luciferase activity is directly related to Gli promoter activation, and indicates stimulation of the Hh pathway by conditioned media or SAG. Data represent mean \pm SEM of experiments performed in triplicate (n = 3).



Supplementary Figure S2. Effect of RUSKI inhibitors on viability of Shh-Light2 cells. Shh-Light2 cells were plated at 10×10^3 cells/well of a 96-well plate, incubated overnight and treated the following day with RUSKI-41 (blue), RUSKI -43 (red), RUSKI-201 (green) (0.5 to 25 μ M) or DMSO vehicle for 48 h. Viability was measured using the Cyquant Direct Cell Proliferation Assay, and response normalized to vehicle control. Data represent mean \pm SEM of experiments performed at least in triplicate ($n \geq 4$).

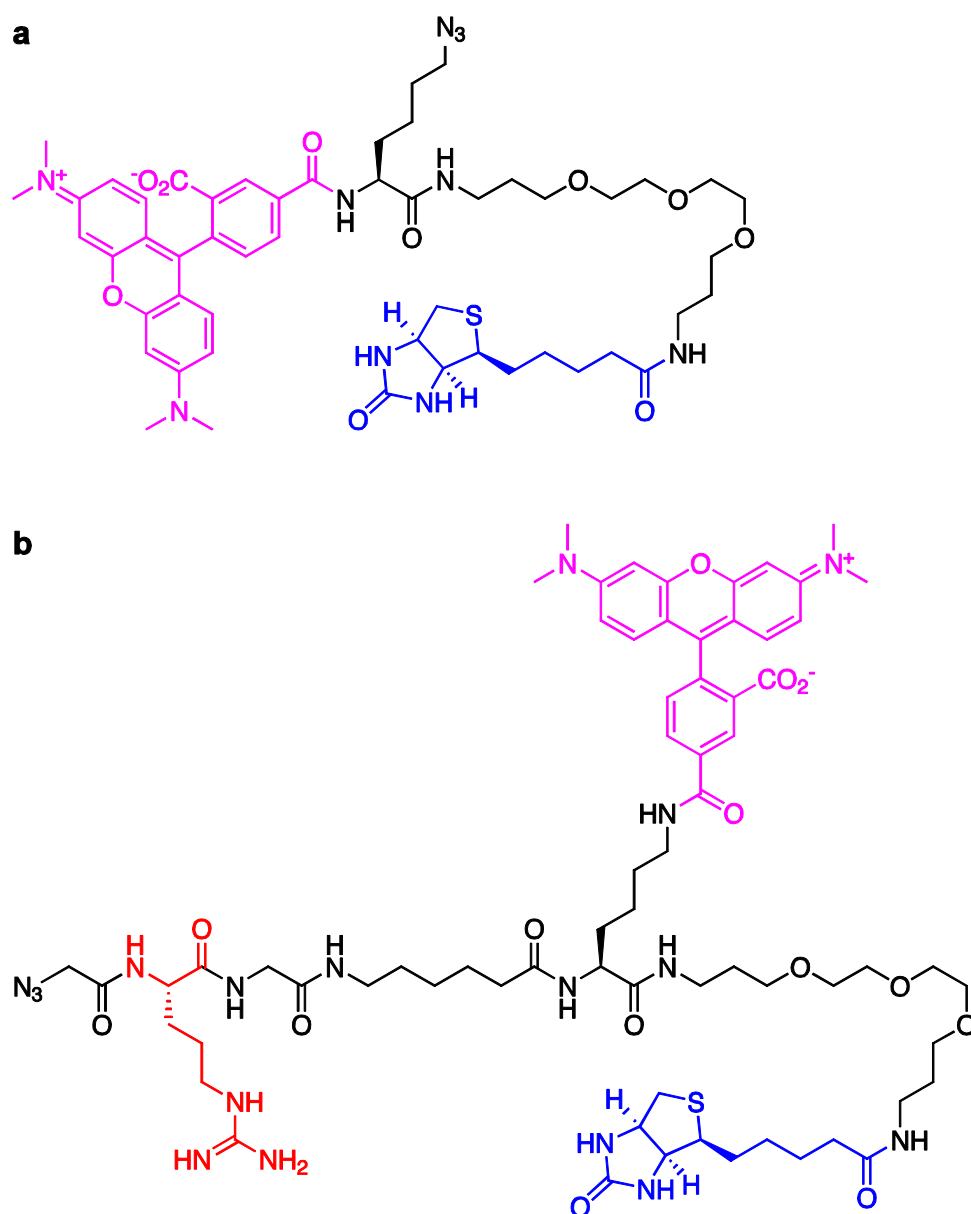


Supplementary Figure S3. Effect of RUSKI inhibitors on *Renilla* luciferase activity. The effects of RUSKI-41 (blue), RUSKI-43 (red), and RUSKI-201 (green) on *Renilla* luciferase activity were characterized as described in Materials and Methods. (a) Addition of inhibitors to HEK-293 Shh⁺ and subsequent transfer of conditioned medium to Shh-Light2 reporter cells. (b) Addition of inhibitors to pre-conditioned medium and subsequent transfer to Shh-Light2 reporter cells. (c) Addition of inhibitors to SAG-containing medium prior to transfer to Shh-Light2 reporter cells. *Renilla* luciferase activity corresponding to the Shh-Light2 firefly luciferase data (**Figure 2**) are shown (a-c). To determine the overall effect of each compound on *Renilla* luciferase activity, the mean across all conditions was calculated for (d) RUSKI-41, (e) RUSKI-43, and (f) RUSKI-201. RUSKI-41 significantly inhibited *Renilla* luciferase activity at 10 μ M ($p < 0.05$, $n = 14$), while RUSKI-43 had a significant effect at 5 μ M and 10 μ M ($p < 0.0001$, $n = 18$); RUSKI-201 had no significant effect. Data represent mean \pm SEM of experiments performed in triplicate ($n \geq 3$).

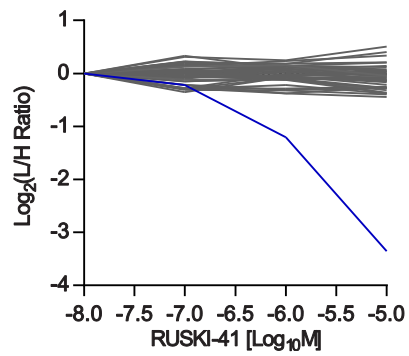


Supplementary Figure S4. Effect of RUSKI-43, RUSKI-201 and LGK974 on Wnt signaling.

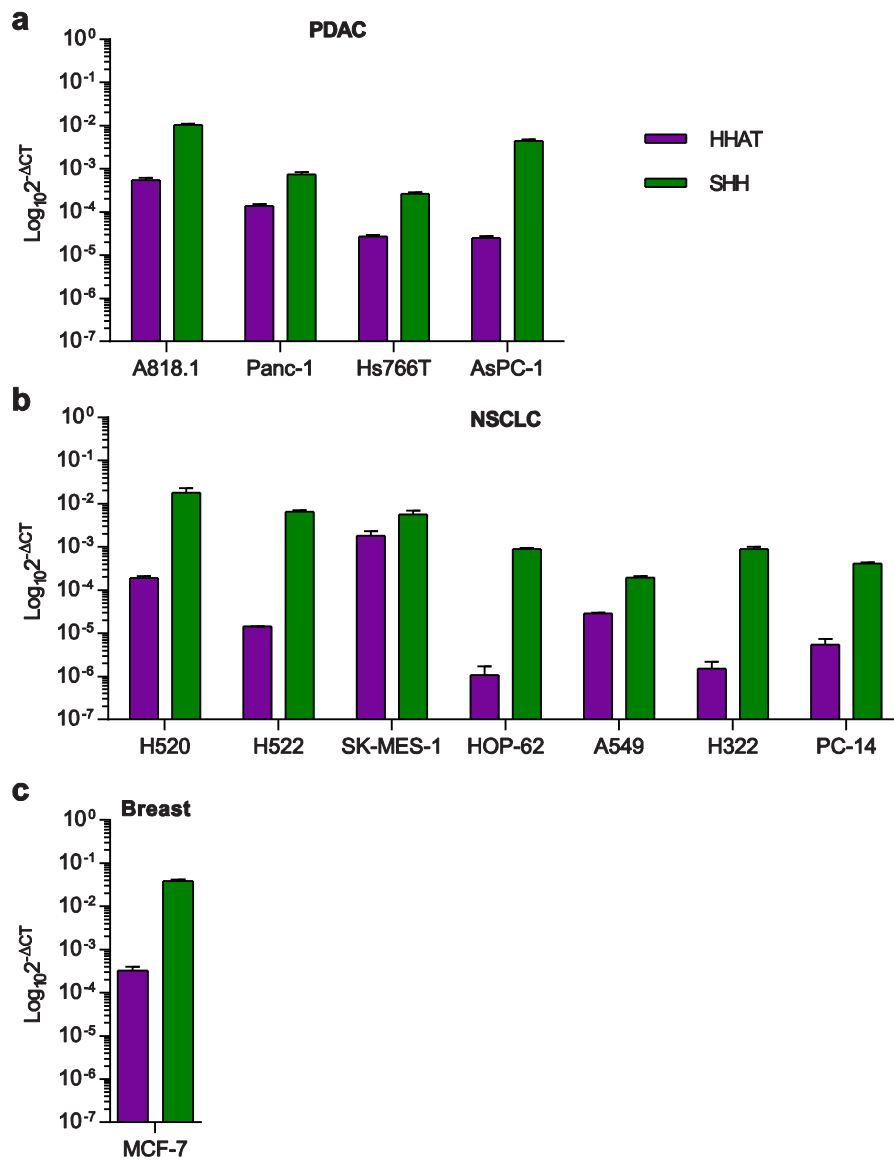
Assays were performed as described in Materials and Methods. (a) Structure of Porcupine inhibitor LGK974.² (b) Normalized luciferase activity showing inhibition of Wnt signaling by RUSKI-43 and LGK974 ($p < 0.0001$), whereas RUSKI-201 did not have a statistically significant effect on signaling. (c) Normalized *Renilla* activity showing no compound had a statistically significant effect on cell growth. Data represent mean \pm SEM of experiments performed in triplicate ($n \geq 2$).



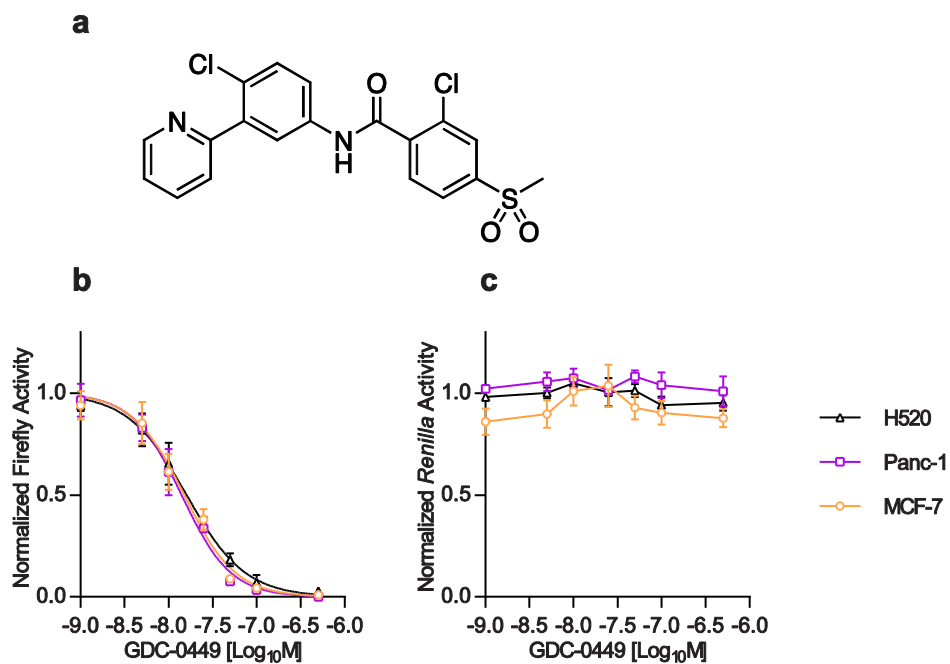
Supplementary Figure S5. Structure of bioorthogonal capture reagents. (a) Azido-TAMRA-PEG₃-biotin (AzTB) trifunctional capture reagent,³ allowing for isolation through a biotin tag (blue) or detection *via* in-gel fluorescence of the TAMRA fluorophore (pink) as employed in WB tagging experiments (**Figure 3a and 3b**). Azido-arginine-TAMRA-PEG₃-biotin (AzRTB) tetrafunctional capture reagent,⁴ allowing for detection *via* in-gel fluorescence of the TAMRA fluorophore (pink), isolation through a biotin tag (blue), and release from the affinity resin *via* trypsin cleavage C-terminal of the arginine residue (red) as employed in quantitative proteomics experiments (**Figure 3c and 3d**).



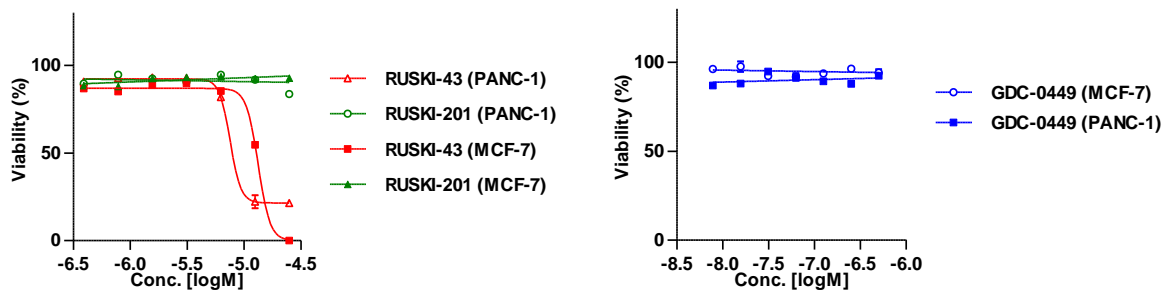
Supplementary Figure S6. Chemoproteomic profiling of the effect of RUSKI-41 treatment on protein palmitoylation. Change in L/H ratio upon RUSKI-41 treatment from spike-in SILAC quantitative proteomics were measured as described in Materials and Methods. Each line represents a protein known to be palmitoylated, normalized to inhibitor vehicle control. The blue line represents Hh proteins (Shh, Dhh, Ihh) (n = 3). Data represent mean \pm SEM of experiments performed in duplicate.



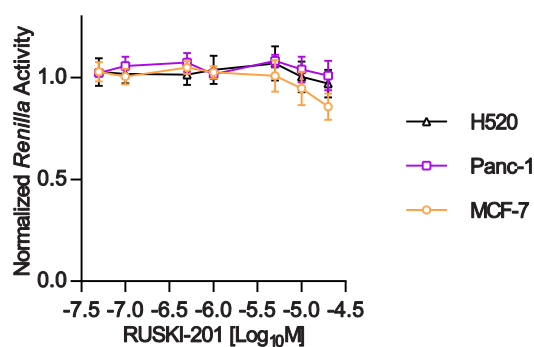
Supplementary Figure S7. Expression of HHAT and SHH in pancreatic, lung and breast tumor cell lines. (a) Pancreatic (PDAC), (b) lung (NSCLC) and (c) breast cancer cell lines were plated in duplicate in 6-well plates and harvested into TRIzol 24 h later, at approximately 80% confluence. Following RNA extraction and cDNA synthesis, samples were assessed for expression of HHAT (purple bars) and SHH (green bars) genes using quantitative real-time PCR. Expression of each gene was normalized to GAPDH, and relative expression values are shown (n ≥ 3).



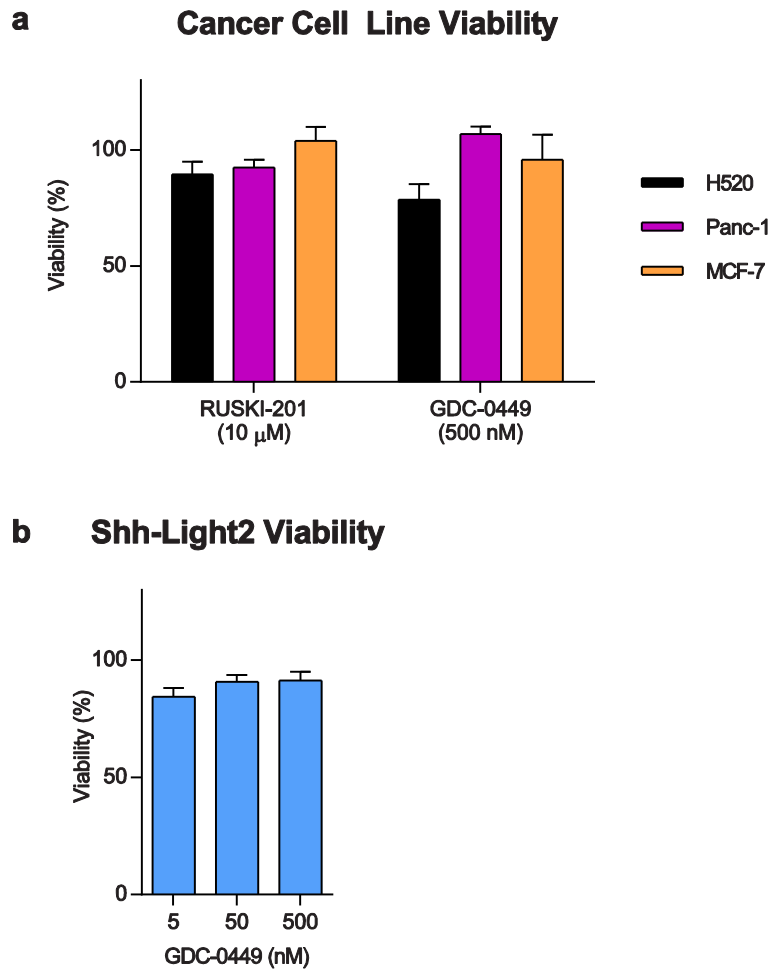
Supplementary Figure S8. Effect of Smo inhibitor GDC-0449 on Hh signaling induced by tumor cell lines. (a) Structure of Smo inhibitor GDC-0449. (b) H520 (black), Panc-1 (purple) and MCF-7 (orange) cell lines were co-cultured with Shh-Light2 cells by combining 2.5×10^3 tumor cells with 10×10^3 reporter cells per well of a 96-well plate. After visual evidence of cell attachment (4-5 h after seeding) co-cultures were treated with GDC-0449 (1-500 nM) or vehicle. After 48 h cells were lysed and firefly and (c) *Renilla* luciferase activities recorded, and responses normalized to vehicle control. Data demonstrate that an on-target Hh pathway inhibitor exhibits dose-dependent inhibition of firefly luciferase with no effect on *Renilla* luciferase. Data represent mean \pm SEM of experiments performed at least in triplicate ($n \geq 3$).



Supplementary Figure S9. Effect of GDC-0449, RUSKI-43, and RUSKI-201 on the viability of Panc-1 and MCF-7 cells. Panc-1 and MCF-7 cells were plated at 1×10^4 cells/well and 5×10^3 cells/well, respectively, and treated with RUSKI-43 (red), RUSKI-201 (green), or GDC-0449 (blue) for 48 h. Cell viability was quantified using the CellTiter-Glo Viability assay and responses were normalized to vehicle control and Puromycin treated samples. RUSKI-43: $EC_{50} = 7.4 \pm 0.49 \mu\text{M}$ (Panc-1) and $13.3 \pm 0.27 \mu\text{M}$ (MCF-7).



Supplementary Figure S10. Effect of RUSKI-201 on *Renilla* luciferase activity of Shh-Light2 cells co-cultured with cancer cell lines. H520 (black), Panc-1 (purple) and MCF-7 (orange) tumor cell lines were co-cultured with Shh-Light2 cells by combining 2.5×10^3 tumor cells with 10×10^3 reporter cells per well of a 96-well plate. After visual evidence of cell attachment (4-5 h after seeding) co-cultures were treated with RUSKI-201 (0.05-20 μ M) or vehicle. After 48 h cells were lysed and firefly and *Renilla* luciferase activities recorded, and response normalized to vehicle control. *Renilla* luciferase activity indicates RUSKI-201 does not exhibit cytotoxic effects, and correspondingly exhibits dose-dependent inhibition of firefly luciferase (**Figure 4a**). Data represent mean \pm SEM of experiments performed at least in triplicate ($n \geq 3$).



Supplementary Figure S11. Effect of RUSKI-201 and GDC-0449 on cell viability. (a) Effect of RUSKI-201 and GDC-0449 on viability of cancer cell lines. H520 (black), Panc-1 (purple) and MCF-7 (orange) were plated at 5×10^3 cells/well of a 96-well plate and treated the following day with either RUSKI-201 (10 μ M) or GDC-0449 (500 nM) for 48 h. Viability was measured using the CyQuant Direct Cell Proliferation Assay. Neither compound exhibited a significant effect on viability. Data represent mean \pm SEM of experiments performed at least in triplicate ($n \geq 3$). (b) Effect of GDC-0449 on the viability of Shh-Light2 cells. Shh-Light2 cells were plated at 10×10^3 cells/well of a 96-well plate and treated the following day with GDC-0449 (5-500 nM) for 48 h. Viability was measured using the CyQuant Direct Cell Proliferation Assay. GDC-0449 had no significant effect on viability. Data represent mean \pm SEM of experiments performed at least in triplicate ($n = 2$).

SUPPLEMENTARY TABLES

Supplementary Table S1. Palmitoylated proteins identified by YnPal-tagging in response to RUSKI-201 treatment using spike-in SILAC-based quantitative proteomics.

Gene Name	Protein names	Peptides	Log ₂ L/H (ratio)			
			RUSKI-201 (μM)			
			0.1	0.5	1.0	10.0
ACTG1	Actin, cytoplasmic 2;Actin, cytoplasmic 2, N-terminally processed	7	-0.36	-0.42	-0.38	-0.33
ALDOA	Fructose-bisphosphate aldolase A;Fructose-bisphosphate aldolase	10	-0.18	-0.32	-0.42	-0.39
ANXA1	Annexin A1;Annexin	3	-0.24	-0.36	-0.17	-0.34
ANXA2;ANXA2P2	Annexin A2;Annexin;Putative annexin A2-like protein	24	-0.37	0.17	-0.06	0.57
ATP11B	Probable phospholipid-transporting ATPase 1F	9	-0.25	-0.39	-0.44	-0.16
ATP13A3	Probable cation-transporting ATPase 13A3	3	-0.15	-0.33	-0.04	-0.34
ATP1A1	Sodium/potassium-transporting ATPase subunit alpha-1	8	-0.41	-0.36	-0.31	-0.16
ATP6V0A2	V-type proton ATPase 116 kDa subunit a isoform 2	15	-0.64	-0.76	-0.46	-0.59
BCAM	Basal cell adhesion molecule	3	0.30	0.30	0.24	0.19
CAND1	Cullin-associated NEDD8-dissociated protein 1	4	-0.36	-0.46	-0.34	-0.42
CANX	Calnexin	13	-0.30	-0.19	0.05	-0.23
CAV1	Caveolin-1;Caveolin	4	-0.57	-0.59	-0.51	-1.01
CCT2	T-complex protein 1 subunit beta	4	-0.42	-0.42	-0.50	-0.42
CCT3	T-complex protein 1 subunit gamma	9	-0.26	-0.42	-0.19	-0.33
CCT4	T-complex protein 1 subunit delta	4	-0.32	-0.38	-0.42	-0.35
CCT6A	T-complex protein 1 subunit zeta	4	-0.33	-0.54	-0.29	-0.46
CCT8	T-complex protein 1 subunit theta	5	-0.34	-0.44	-0.39	-0.50
CD151	CD151 antigen	2	0.12	0.21	0.20	-0.22
CD276	CD276 antigen	10	-0.20	-0.41	-0.26	-0.22
CD44	CD44 antigen	27	-0.33	-0.38	-0.09	-0.38
CD81	CD81 antigen	9	-0.20	-0.29	-0.13	-0.39
CD9	CD9 antigen	3	-0.25	-0.33	-0.20	-0.39
CFL1	Cofilin-1	9	-0.14	-0.17	0.03	-0.06
CPD	Carboxypeptidase D	4	-0.44	-0.57	-0.43	-0.52
CSE1L	Exportin-2	5	-0.32	-0.51	-0.35	-0.47
CTLC	Clathrin heavy chain 1	8	-0.36	-0.26	-0.25	-0.33
CXADR	Coxsackievirus and adenovirus receptor	6	-0.44	-0.35	-0.27	-0.58
DAGLB	Sn1-specific diacylglycerol lipase beta	7	-0.33	-0.40	-0.23	-0.20
EEF1A1;EEF1A1P5;EEF1A2	Elongation factor 1-alpha 1;Putative elongation factor 1-alpha-like 3;Elongation factor 1-alpha 2	5	-0.15	-0.25	-0.04	-0.12
EEF1G	Elongation factor 1-gamma	2	-0.37	-0.48	-0.40	-0.47
ENO1	Alpha-enolase	15	-0.15	-0.21	-0.13	-0.31
ERGIC2	Endoplasmic reticulum-Golgi intermediate compartment protein 2	9	-0.40	-0.58	-0.33	-0.42
FLOT1	Flotillin-1	7	-0.55	-0.63	-0.42	-0.41
GAPDH	Glyceraldehyde-3-phosphate dehydrogenase	3	-0.29	0.02	-0.10	0.07

Gene Name	Protein names	Peptides	Log ₂ L/H (ratio)			
			RUSKI-201 (µM)			
			0.1	0.5	1.0	10.0
GLO1	Lactoylglutathione lyase	2	-0.64	-0.65	-0.38	-0.73
GNA11;GNAQ	Guanine nucleotide-binding protein subunit alpha-11	4	-0.30	-0.34	-0.32	-0.32
GNA13	Guanine nucleotide-binding protein subunit alpha-13	2	0.07	0.08	0.18	0.36
GOLIM4	Golgi integral membrane protein 4	2	-0.20	-0.28	-0.05	-0.35
GPI	Glucose-6-phosphate isomerase	11	-0.09	-0.21	-0.01	-0.17
GSTP1	Glutathione S-transferase P	2	-0.37	-0.45	-0.37	-0.20
HSP90AA1	Heat shock protein HSP 90-alpha	6	-0.38	-0.48	-0.36	-0.47
HSP90AB1	Heat shock protein HSP 90-beta	5	-0.22	-0.29	-0.27	-0.32
HSPA1A	Heat shock 70 kDa protein 1A/1B	4	-0.15	-0.33	-0.26	-0.32
HSPA8	Heat shock cognate 71 kDa protein	16	-0.14	-0.36	-0.11	-0.29
HSPD1	60 kDa heat shock protein, mitochondrial	8	-0.27	-0.34	-0.19	-0.32
IPO5	Importin-5	12	-0.37	-0.41	-0.27	-0.47
KPNB1	Importin subunit beta-1	7	-0.35	-0.48	-0.34	-0.44
LDHA	L-lactate dehydrogenase A chain	15	-0.23	-0.40	-0.28	-0.50
LDHB	L-lactate dehydrogenase B chain;L-lactate dehydrogenase	4	-0.25	-0.30	-0.25	-0.48
LNPEP	Leucyl-cystinyl aminopeptidase;Leucyl-cystinyl aminopeptidase, pregnancy serum form	3	-0.43	-0.51	-0.28	-0.35
LSR	Lipolysis-stimulated lipoprotein receptor	9	-0.02	-0.07	-0.06	-0.14
MDH2	Malate dehydrogenase, mitochondrial;Malate dehydrogenase	3	-0.11	-0.10	0.00	0.00
NCAM1	Neural cell adhesion molecule 1	10	-0.12	-0.16	-0.08	-0.20
NPC1	Niemann-Pick C1 protein	3	-0.11	-0.22	0.01	-0.19
PFN1	Profilin-1	4	-0.45	-0.53	-0.53	-0.53
PHGDH	D-3-phosphoglycerate dehydrogenase	2	-0.48	-0.56	-0.30	-0.43
PI4K2A	Phosphatidylinositol 4-kinase type 2-alpha	2	-0.33	-0.48	-0.29	-0.69
PI4K2B	Phosphatidylinositol 4-kinase type 2-beta	2	-0.12	-0.49	-0.20	-0.41
PKM2	Pyruvate kinase isozymes M1/M2;Pyruvate kinase	14	-0.33	-0.34	-0.28	-0.35
PLS3	Plastin-3	12	-0.06	-0.18	-0.32	-0.40
PLSCR1	Phospholipid scramblase 1	7	-0.17	-0.27	-0.05	-0.76
PLSCR1	Phospholipid scramblase 1	7	-0.32	-0.34	-0.12	-1.10
PPIA	Peptidyl-prolyl cis-trans isomerase A;Peptidyl-prolyl cis-trans isomerase	7	-0.10	-0.10	-0.04	-0.12
PPP2R1A	Serine/threonine-protein phosphatase 2A 65 kDa regulatory subunit A alpha isoform	17	-0.40	-0.52	-0.39	-0.38
PRDX1	Peroxiredoxin-1	2	-0.16	-0.19	-0.16	-0.34
PRKDC	DNA-dependent protein kinase catalytic subunit	5	-0.45	-0.29	-0.35	-0.38
PTK7	Inactive tyrosine-protein kinase 7	12	-0.58	-0.63	-0.37	-0.46
PTPLAD1	3-hydroxyacyl-CoA dehydratase 3	6	-0.17	-0.27	-0.18	-0.24
PTRH2	Peptidyl-tRNA hydrolase 2, mitochondrial	2	-0.58	-0.55	-0.49	-0.45
RPL13	60S ribosomal protein L13	4	0.40	0.36	0.37	0.38
RPL15	60S ribosomal protein L15;Ribosomal protein L15	6	0.05	0.04	0.02	0.05
RPL6	60S ribosomal protein L6	4	0.61	0.52	0.61	0.52

Gene Name	Protein names	Peptides	Log ₂ L/H (ratio)			
			RUSKI-201 (μM)			
			0.1	0.5	1.0	10.0
RPL7	60S ribosomal protein L7	4	-0.27	-0.11	-0.03	-0.16
RPS2	40S ribosomal protein S2	7	-0.23	-0.26	-0.09	-0.40
RPS3	40S ribosomal protein S3	14	-0.31	-0.29	-0.32	-0.23
RPS3A	40S ribosomal protein S3a	13	0.01	-0.01	0.18	-0.06
RPS4X	40S ribosomal protein S4, X isoform	2	0.28	0.37	0.87	0.58
RPS9	40S ribosomal protein S9	5	-0.16	-0.17	-0.24	-0.26
SCAMP3	Secretory carrier-associated membrane protein 3	2	-0.28	-0.29	0.06	-0.17
SCARB2	Lysosome membrane protein 2	2	-0.10	-0.24	0.08	-0.18
SCRIB	Protein scribble homolog	5	-0.26	-0.32	-0.14	-0.09
SHH	Sonic hedgehog protein;Sonic hedgehog protein N-product;Sonic hedgehog protein C-product;Indian hedgehog protein;Indian hedgehog protein N-product;Indian hedgehog protein C-product	5	-0.74	-1.20	-1.43	-3.25
SLC1A5	Neutral amino acid transporter B(0)	6	-0.42	-0.44	-0.28	-0.44
SLC25A5	ADP/ATP translocase 2	2	-0.21	-0.23	-0.10	-0.17
SLC35B2	Adenosine 3-phospho 5-phosphosulfate transporter 1	5	-0.10	-0.07	0.02	-0.10
SLC38A2	Sodium-coupled neutral amino acid transporter 2	3	-0.38	-0.62	-0.29	-0.42
SLC44A1	Choline transporter-like protein 1	4	-0.24	-0.30	0.01	-0.30
SLC7A1	High affinity cationic amino acid transporter 1	2	-0.29	-0.41	-0.01	-0.29
SNAP23	Synaptosomal-associated protein 23;Synaptosomal-associated protein	9	-0.43	-0.29	-0.14	-0.21
STX12	Syntaxin-12	2	-0.69	-0.84	-0.57	-0.85
STX8	Syntaxin-8	3	-0.48	-0.52	-0.38	-0.41
TCP1	T-complex protein 1 subunit alpha	11	-0.22	-0.40	-0.28	-0.32
TFRC	Transferrin receptor protein 1;Transferrin receptor protein 1, serum form	5	-0.39	-0.32	-0.25	-0.11
TKT	Transketolase	4	-0.16	-0.44	-0.30	-0.17
TPI1	Triosephosphate isomerase	6	-0.09	-0.20	0.00	-0.16
TUBB	Tubulin beta chain	9	-0.20	-0.28	-0.12	-0.33
TUBB4B;TUBB3	Tubulin beta-4B chain	2	-0.01	-0.22	-0.09	-0.14
UBA1	Ubiquitin-like modifier-activating enzyme 1	7	-0.26	-0.40	-0.29	-0.36
VAMP3;VAMP2	Vesicle-associated membrane protein 3;Vesicle-associated membrane protein 2	7	0.00	-0.15	-0.08	-0.35
VAMP7	Vesicle-associated membrane protein 7	4	-0.30	-0.22	-0.01	-0.18
VCP	Transitional endoplasmic reticulum ATPase	3	-0.47	-0.63	-0.57	-0.49
VDAC2	Voltage-dependent anion-selective channel protein 2	7	-0.26	-0.30	-0.19	-0.33
XPO1	Exportin-1	7	-0.44	-0.50	-0.38	-0.41
YWHAE	14-3-3 protein epsilon	18	-0.10	-0.26	-0.12	-0.28
YWHAZ	14-3-3 protein zeta/delta	7	-0.23	-0.28	-0.12	-0.11

Supplementary Table S2. Palmitoylated proteins identified by YnPal-tagging in response to RUSKI-41 treatment using spike-in SILAC-based quantitative proteomics.

Gene Name	Protein names	Peptides	Log ₂ L/H (ratio) RUSKI-41 (μM)		
			0.1	1.0	10.0
ACACA	Acetyl-CoA carboxylase 1;Biotin carboxylase	18	0.04	0.10	-0.16
ALDOA	Fructose-bisphosphate aldolase A;Fructose-bisphosphate aldolase	13	-0.15	-0.12	-0.09
CANX	Calnexin	12	0.14	0.23	0.34
CAV1	Caveolin-1;Caveolin	5	-0.01	-0.12	-0.37
CD276	CD276 antigen	8	0.02	0.08	-0.01
CD44	CD44 antigen	28	0.01	-0.08	-0.28
CD63	CD63 antigen	8	-0.07	-0.03	0.03
CD9	CD9 antigen	4	0.08	-0.02	-0.02
CKAP4	Cytoskeleton-associated protein 4	1	-0.31	-0.32	-0.39
CXADR	Coxsackievirus and adenovirus receptor	7	0.13	0.16	-0.05
DNAJC5	DnaJ homolog subfamily C member 5	2	-0.28	-0.01	-0.09
EEF1A1;EEF1A1P5;EEF1A2	Elongation factor 1-alpha 1;Putative elongation factor 1-alpha-like 3;Elongation factor 1-alpha 2	5	-0.12	-0.11	-0.32
EEF2	Elongation factor 2	6	0.02	-0.05	-0.21
ENO1	Alpha-enolase	13	0.33	0.09	0.00
ERGIC2	Endoplasmic reticulum-Golgi intermediate compartment protein 2	9	-0.05	-0.11	-0.28
GAPDH	Glyceraldehyde-3-phosphate dehydrogenase	4	-0.07	-0.06	0.05
GNA11	Guanine nucleotide-binding protein subunit alpha-11	8	0.21	0.18	0.40
HSP90AB1;HSP90AB3P;HSP90AB2P	Heat shock protein HSP 90-beta	5	-0.16	-0.06	-0.12
HSPA1A	Heat shock protein HSP 90-alpha	3	0.05	-0.07	-0.12
HSPD1	60 kDa heat shock protein, mitochondrial	8	0.23	0.14	0.12
KPNB1	Importin subunit beta-1	8	-0.29	-0.08	-0.07
LDHA	L-lactate dehydrogenase A chain	18	0.22	0.07	0.14
LDHB	L-lactate dehydrogenase B chain;L-lactate dehydrogenase	8	0.02	0.05	-0.02
NCAM1	Neural cell adhesion molecule 1	10	-0.04	0.02	-0.05
PLSCR1	Phospholipid scramblase 1	7	0.15	0.05	-0.14
PVR	Poliovirus receptor	4	0.00	0.12	-0.01
RPL13	60S ribosomal protein L13	5	-0.22	-0.38	-0.26
RPL6	60S ribosomal protein L6	7	-0.28	-0.38	-0.45
RRAS2	Ras-related protein R-Ras2	9	-0.10	0.15	0.20
SHH;IHH	Sonic hedgehog protein;Sonic hedgehog protein N-product;Sonic hedgehog protein C-product;Indian hedgehog protein;Indian hedgehog protein N-product;Indian hedgehog protein C-product	5	-0.22	-1.21	-3.35
SLC1A5	Neutral amino acid transporter B(0)	6	0.08	0.13	0.05
SLC25A5;SLC25A6;SLC25A4	Neutral amino acid transporter B(0)	5	-0.35	-0.07	-0.38
SLC35B2	Adenosine 3-phospho 5-phosphosulfate transporter 1	5	0.19	0.19	0.21
SLC38A1	Sodium-coupled neutral amino acid transporter 1	2	-0.07	0.14	0.03
SLC38A2	Sodium-coupled neutral amino acid transporter 2	4	0.17	0.13	0.08
STOM	Erythrocyte band 7 integral membrane protein	3	0.32	0.25	0.51
TFRC	Transferrin receptor protein 1;Transferrin receptor protein 1, serum form	8	0.00	-0.06	-0.16
TP1	Triosephosphate isomerase	6	-0.28	-0.29	-0.25
TUBB4B;TUBB;TUBB2A;TUBB2B;TUBB	Tubulin beta-4B chain	19	-0.29	-0.22	-0.37
YWHAE	14-3-3 protein epsilon	9	0.05	-0.09	-0.13
YWHAZ	14-3-3 protein zeta/delta	11	-0.21	-0.31	-0.28

MATERIALS AND METHODS

Reagents

All reagents were purchased from Sigma-Aldrich (Gillingham, Kent, UK) and used without further purification, unless otherwise stated. GDC-0449 was purchased from Selleck Chemicals (Munich, Germany). Smoothed Agonist (SAG) was purchased from Calbiochem/Merck Millipore (Watford, Hertfordshire, UK).

Chemical Synthesis

RUSKI inhibitors were synthesized and characterized as previously described.⁵⁻⁷ Heptadec-16-ynoic acid (YnPal) was synthesized as previously described.³ AzTB and AzRB were synthesized as previously described.^{3,4} LGK974 was a kind gift from Prof. Lawrence Lum.²

Cell Lines and Tissue Culture Reagents

HEK-293a cells stably transfected with *SHH* (HEK-293 Shh⁺ cells) were maintained as previously described.⁸ Shh-Light2 cells⁹ were a generous gift from Dr. Suzanne Eaton (Max Planck Institute for Cell Biology and Genetics, Dresden, Germany) and maintained in DMEM supplemented with 10% FBS, 400 µg/mL G418 (geneticin) and 150 µg/mL Zeocin (Invitrogen). Mouse L cells stably transfected with Wnt luciferase reporters¹⁰ were a kind gift from Prof. Lawrence Lum (UT Southwestern Medical Center, Dallas, Texas) and maintained in high glucose DMEM (4.5 g/L) supplemented with 10% FBS. Human pancreatic ductal adenocarcinoma Panc-1 cells (ATCC, CRL-1469) were maintained in DMEM with 10% FBS. Lung squamous cell carcinoma H520 cells (ATCC, HTB-182) were maintained in RPMI-1640 medium (Invitrogen) with 10% FBS. Human breast adenocarcinoma MCF-7 cells (ATCC, HTB-22) were maintained in Eagle's Minimum Essential Medium (ATCC, EMEM) with 10% FBS. ATCC cancer cell lines were purchased from LGC Standards (Teddington, Middlesex, UK). All cell lines were maintained at 37 °C, 5% CO₂ under humidified conditions.

Shh-Light2 Assay

Shh-Light2 cells are mouse NIH-3T3 cells stably transfected to express firefly luciferase under a Gli-inducible promoter, and constitutively expressing *Renilla* luciferase.⁹

Inhibition of media conditioning by RUSKI compounds

HEK-293 Shh⁺ cells were plated at 1.2×10^5 cells/well of a 12-well plate (Nunc) in DMEM supplemented with 3% FBS and allowed to adhere overnight. Cells were treated the following day with DMEM supplemented with 3% FBS containing either DMSO vehicle or RUSKI inhibitor (0.5-10 µM). After 24 h, the conditioned medium was centrifuged (2,000 rpm, 3 min), and the supernatant (100 µL conditioned medium/well) added to Shh-Light2 cells plated 24 h previously at 2×10^4 cells/well of a 96-well plate (Nunc) in DMEM supplemented with 3% FBS. Shh-Light2 cells were incubated for 48 h. Luciferase activity was measured using the Dual-Luciferase reporter system (Promega Corporation, Madison, WI, USA), according to the manufacturer's instructions. Briefly, cells were washed twice in 1 × phosphate buffered saline (PBS), then lysed with lysis buffer (20 µL/well) for 30 min with shaking. The cell lysate (5 µL/well) was added to a 96-well black assay plate (Corning)

followed by addition of firefly luciferase assay reagent II (20 μ L/well) and luminescence recorded for 2 sec/well. After luciferase measurement, activity was quenched and *Renilla* luciferase recorded for 2 sec/well following the addition of Stop&Glo reagent (20 μ L/well). Luminescence was measured in a Lumimark luminometer (Bio-Rad, Richmond, CA, USA), and response normalized to vehicle control. Experiments were performed in triplicate, at least three times per condition and compound.

Off-target effects of RUSKI compounds on Shh-Light2 cells

HEK-293 Shh⁺ cells were plated as described and medium refreshed the following day without addition of compounds or vehicle. Conditioned medium was collected after 24 h and centrifuged as previously described. DMSO vehicle or RUSKI compounds (0.5-10 μ M) were added to the supernatant, and the pre-conditioned medium used to treat Shh-Light2 cells. Luciferase activity was recorded as previously described. Experiments were performed in triplicate, at least three times per condition and compound.

Recovery of canonical Hh signaling by SAG

Shh-Light2 cells were plated as previously described and incubated overnight. Medium was refreshed with DMEM supplemented with 3% FBS containing SAG (1 nM) followed by incubation for 1 h. RUSKI compounds (0.5-10 μ M) were then added followed by incubation for 1 h. Luciferase activity was recorded as previously described. Experiments were performed in triplicate, at least three times per compound.

Co-culture of cancer cell lines

Panc-1, H520 and MCF-7 cancer cell lines were co-cultured with Shh-Light2 cells at 2.5×10^3 cells/well and 10×10^3 cells/well, respectively, in DMEM containing 3% FBS (100 μ L/well). Cell mixtures were allowed to adhere for approximately 5 h before addition of test compounds. RUSKI-201 (0.5-10 μ M) or GDC-0449 (1-500 nM) were incubated with the cells for 48 h before cell lysis and measurement of luciferases as described previously. Experiments were performed at least in triplicate, at least three times per compound.

Wnt signaling assay

Mouse L cells stably transfected with a Wnt/ β -catenin pathway-responsive firefly luciferase reporter plasmid (SuperTopFlash or STF), a constitutive *Renilla* luciferase control reporter, and a Wnt3A expression construct.¹⁰ Cells were plated at 4×10^4 cells/well of a 96-well plate (Nunc) and cultured for 24 h as described. Cells were washed twice with PBS and treated with high glucose DMEM supplemented with 10% FBS containing either DMSO vehicle, RUSKI inhibitor (10 μ M) or LGK974 (100 nM). After 48 h, cells were washed twice with PBS, then processed for luciferase activity as previously described. Luminescence was recorded in 96-well white assay plate (Corning) on a SpectraMax M2e Multimode Microplate Reader (Molecular Devices, Sunnyvale, CA, USA), and response normalized to vehicle control. Experiments were performed in triplicate, at least twice per compound.

Cell viability assays

CyQUANT direct cell proliferation assay

Shh-Light2 cells were plated at 1×10^4 cells/well in DMEM supplemented with 3% FBS. Cells were incubated overnight then treated with either DMSO vehicle, RUSKI compounds (0.5-25 μ M), or GDC-0449 (5-500 nM) for 48 h. Cells were assessed for viability using the CyQUANT Direct Cell Proliferation assay (Life Technologies Ltd., Paisley, UK) according to the manufacturer's instructions, with the following modifications. Briefly, medium was exchanged for 200 μ L/well of $1 \times$ detection reagent (DMEM supplemented with CyQUANT Direct Nucleic Acid Stain (0.05% final concentration) and CyQUANT Direct background suppressor (0.25% final concentration)), and incubated for 2 h at 37 °C. Fluorescence was detected using an M2e SpectraMax spectrometer (Molecular Devices, Sunnyvale, CA, USA) with an excitation wavelength of 485 nm and an emission wavelength of 538 nm and response normalized to vehicle control. Experiments were performed in triplicate, at least three times per compound.

Panc-1, H520 and MCF-7 were plated at 5×10^3 cells/well in DMEM, RPMI-1640 or EMEM, respectively, supplemented with 3% FBS. Cells were incubated overnight then treated with GDC-0449 (500 nM) or RUSKI-201 (10 μ M) for 48 h. Viability was measured as previously described and response normalized to vehicle control. Experiments were performed in triplicate, at least three times per compound.

CellTiter-Glo viability assay

Panc-1 and MCF-7 cells were plated at 1×10^4 cells/well and 5×10^3 cells/well, respectively, in 50 μ L DMEM per well supplemented with 10% FBS. Cells were incubated overnight then treated with 50 μ L of either Puromycin (2 μ g/mL), DMSO vehicle, RUSKI compounds (25-0.4 μ M), or GDC-0449 (500-8 nM) in DMEM supplemented with 10% FBS for 48 h. Cells were assessed for viability using the CellTiter-Glo Viability Assay (Promega, Southampton, UK) according to the manufacturer's instructions. Briefly, 100 μ L of the CellTiter-Glo reagent were added to each well of the pre-equilibrated plate (30 min at RT). Subsequently the contents were mixed on an orbital shaker at RT for 2 min and the plate was further incubated at RT for another 10 min. Afterwards the luminescence was recorded using a SpectraMax M2e Multimode Microplate Reader and the responses were normalized to vehicle control and the Puromycin treated samples.

In vitro palmitoylation, bioorthogonal ligation and western blotting

HEK-293 Shh⁺ cells were plated at 4×10^5 cells/well in a 6-well culture dish and incubated overnight. Culture medium was exchanged to DMEM supplemented with 3% FBS, and cells treated with RUSKI compounds or DMSO vehicle for 1 h. YnPal (20 μ M) was added to the media, and cells incubated for a further 6 h. Cell monolayers were washed twice in PBS at 4 °C, and incubated in lysis buffer (PBS containing 1% Triton X-100, 0.1% SDS and $1 \times$ Complete EDTA-free protease inhibitor cocktail (Roche, Welwyn, UK)) for 15 min. DNA was sheared by passing the lysate through a 0.5 mm (25G) syringe needle three times, and the lysate cleared by centrifugation (16000 \times g, 10 min).

Lysates were quantified using the DC Protein Assay (Bio-Rad) according to the manufacturer's instructions, and the total protein concentration adjusted to 1 mg/mL in lysis buffer prior to copper(I) catalyzed azide-alkyne cycloaddition (CuAAC).^{3,11} Azido-TAMRA-PEG₃-biotin capture reagent (AzTB) (100 μ M), CuSO₄ (1 mM), tris(2-carboxyethyl)phosphine (TCEP) (1 mM), tris[(1-benzyl-1H-1,2,3-triazol-4-yl)methyl]amine (TBTA) (100 μ M) were added to lysates in order, and reactions vortexed for 1 h at RT. EDTA (10 mM) was added to halt the reaction, and proteins precipitated *via* addition of

methanol (4 vol) followed by vortexing for 15 s, then addition chloroform (1 vol) and water (3 vol). Samples were centrifuged (16000 × g, 5 min) and the methanol/water layer removed, followed by washing of the protein pellets with methanol (4 vol) and centrifugation (16000 × g, 5 min). Pellets were washed once more for in-gel fluorescence analysis, or twice more for proteomic analysis. Protein pellets were air-dried briefly then dissolved in 0.2% SDS in 1× PBS to a final concentration of 1 mg/mL. 10 µg of each sample were prepared in 1× NuPAGE loading buffer (Life Technologies) containing 2-mercaptoethanol (10% v/v) and resolved by 15% SDS-PAGE in 1 M Bis Tris buffer, pH 6.7 and fluorescence detected using an Ettan DIGE imager (GE Healthcare).

Following fluorescence visualization, proteins were transferred to PVDF (Immobilon, 0.2 µm pore size, Millipore) using a semi-dry blotter (Hoefer, USA). Shh was detected using rabbit anti-Shh antibody (H160, Santa Cruz Biotechnology, 1:200 dilution), and Tubulin detected using rabbit anti-tubulin antibody (Abcam; 1:10,000 dilution), followed by incubation with goat anti-rabbit-HRP secondary antibody (Southern Biotechnology; 1:25,000 dilution). Visualization was carried out using enhanced chemiluminescence (ECL) reagent (ECL plus, Thermo Fisher Scientific) according to the manufacturer's instructions and detected using an Ettan DIGE imager (GE Healthcare). The Shh tagging ratio (YnPal-Shh/total Shh) was calculated from WB densitometry analysis using ImageQuant (GE Healthcare). Ratios were normalized to YnPal control to generate a tagging IC₅₀ curve. Experiments were performed in duplicate, and repeated six times.

Proteomics

HEK293a cells and HEK-293 Shh⁺ cells were cultured in DMEM containing R10K8 (Arg ¹³C₆, ¹⁵N₄, Lys ¹³C₆, ¹⁵N₂, Dundee Cell Products) supplemented with 10% dialyzed (10,000 mw cut-off) FBS for 3 to 5 passages. R10K8 amino acid-labelled HEK-293 Shh⁺ cells (heavy) were treated with YnPal (20 µM) for 6 h. Unlabelled HEK-293 Shh⁺ cells (light) were treated with RUSKI-41 or RUSKI-201 (0.1 to 10 µM) for 1 h before addition of YnPal (20 µM) and incubation for 6 h. Cell lysates were mixed 1:1 prior to CuAAC functionalization with azido-arginine-PEG₃-biotin (AzRTB) capture reagent as described previously.⁴ After protein precipitation, bioorthogonally ligated proteins (1 mg) were affinity-enriched on NeutrAvidin™ agarose resin (50 µL) (Thermo Fisher Scientific) which had been washed twice with 0.1% SDS in PBS solution prior to use. After gentle shaking for 2 h at room temperature, beads were washed three times with 1% SDS in PBS (10 vol), twice with 4 M urea in 50 mM ammonium bicarbonate (AMBIC) (10 vol) and five times with 50 mM AMBIC (10 vol). Following washing, disulfide bonds were reduced by addition of dithiothreitol (5 µL, 100 mM dithiothreitol in 50 mM AMBIC), followed by brief centrifugation and incubation for 30 min at 55 °C. Beads were washed twice with 50 mM AMBIC (10 vol), and free cysteines alkylated by addition of iodoacetamide (5 µL, 100 mM iodoacetamide) in 50 mM AMBIC, followed by brief centrifugation and incubation in the dark for 30 min at RT. Beads were washed twice with 50 mM AMBIC (10 vol), and enriched samples digested with Trypsin (5 µL, Sequence Grade Modified Trypsin, Promega, stock concentration: 20 µg in 100 µL of 50 mM AMBIC) for 18 h with gentle shaking at 37 °C. Beads were washed with 50 mM AMBIC (80 µL) by vortex-mixing for 10 min. Following brief centrifugation, the supernatant containing digested peptides was collected. Beads were washed again with 0.1% formic acid in dH₂O (80 µL) by vortex-mixing for 10 min, briefly centrifuged and the supernatant collected and combined with the previous supernatant. The combined peptide solutions were desalted following literature protocols.¹² Stage tips were prepared from three layers of C18 Empore disks (3M) cut together using a syringe cutter and fitted into a p200 pipette tip. Stage tips were suspended through the lids of microcentrifuge tubes pierced to the appropriate size. Before introducing samples, stage tips were washed with LCMS grade methanol (150 µL) and MilliQ water (150 µL) followed by centrifugation (2,000 × g, 1 min) per wash. Peptide samples (up to 200 µL) were loaded onto stage tips, the flow-through removed, and stage tips washed with MilliQ water (15 µL). Peptides were eluted into new low protein binding Eppendorf tubes by addition of elution buffer (79% acetonitrile in MilliQ

water). Samples were dried under speed vacuum (Savant DNA 120 concentrator, Thermo Fisher) over approximately 40 min.

Before mass spectrometry analysis, samples were dissolved in proteomic sample buffer (0.5% trifluoroacetic acid, 2% acetonitrile in MilliQ water) (15-30 μ L). Desalted peptides were vortex-mixed for 5 min, centrifuged briefly, sonicated for 20 min, vortex-mixed briefly, centrifuged (7,000 \times g, 10 min, 7 °C) and then transferred to autosampler-compatible vials.

Peptides were separated using a reverse phase Acclaim PepMap RSLC column 50 cm \times 75 μ m inner diameter (Thermo Fisher Scientific) using a 2 h acetonitrile gradient in 0.1% formic acid at a flow rate of 250 nL/min. An Easy nLC-1000 was coupled to a Q Exactive mass spectrometer *via* an easy-spray source (Thermo Fisher Scientific). The Q Exactive was operated in data-dependent mode with survey scans acquired at a resolution of 75,000 at m/z 200 (transient time 256 ms). The 10 most abundant isotope patterns with charge +2 from the survey scan were selected with an isolation window of 3.0 m/z and fragmented by Higher-energy C-trap dissociation (HCD) with normalized collision energies of 25 W. The maximum ion injection times for the survey scan and the MS/MS scans (acquired with a resolution of 17,500 at m/z 200) were 250 and 80 ms, respectively.

Obtained RAW data were processed using MaxQuant software v1.3.0.5. The identified peptides from the MS/MS spectra were searched against the Uniprot database (human proteome and isoforms) using Andromeda search engine. Cysteine carbamidomethylation was selected as a fixed modification, and methionine oxidation as a variable modification. All other parameters were used as default in MaxQuant.

For spike-in SILAC quantitative proteomic analysis in Hhat inhibition assays, data were stringently filtered to require all valid values per protein over three biological replicates and one technical replicate. In order to determine the global palmitoyl proteome profile change upon RUSKI-41 or RUSKI-201 treatment, the light/heavy ratio (L/H, the amount of protein in the lysate with increasing amount of inhibitor/spike-in standard) were converted to \log_2 values and normalized to vehicle control. The \log_2 values of the vehicle control set to 0. For analyzing effects on global palmitoylation, palmitoylated proteins were sorted 1) according to their confidence level (medium to high) from the list of predicted/observed palmitoylated proteins described in SwissPalm (<http://swisspalm.epfl.ch>), Palm CSS (<http://csspalm.biocuckoo.org/index.php>) and Wilson *et al.*¹³ and 2) according to their frequency of occurrence, appearing at least twice out of three biological replicates. In order to determine the tagging IC₅₀ dose-response curves, the L/H values were normalized to vehicle control.

RNA Isolation and quantitative real-time PCR

Cells were plated at 2×10^5 cells/well in 6-well plates (Nunc). After 24 h, RNA was isolated using TRIzol® reagent (Invitrogen) and quantified using a NanoDrop® spectrophotometer (Thermo Scientific). cDNA was synthesized from 250 ng of RNA using the GoScript™ Reverse Transcription System (Promega Corporation), according to the manufacturer's instructions. Intron-spanning primers for *SHH* and *HHAT* were designed using the Universal Probe Library (Roche). The appropriate probe was matched to each set of primers, and used in all PCR reactions. The *GAPDH* gene was used as an endogenous control for normalization, primers for which were purchased from Life Technologies Ltd. Quantitative PCRs were performed and analyzed as described.¹⁴

Software and data analysis

Data analysis (including normalization and Student's t-tests) was performed using Microsoft Excel. Non-linear regression and one-way ANOVA analyses and plotting of data was performed using GraphPad Prism v5.0.

REFERENCES

- (1) Frank-Kamenetsky, M., Zhang, X. M., Bottega, S., Guicherit, O., Wichterle, H., Dudek, H., Bumcrot, D., Wang, F. Y., Jones, S., Shulok, J., Rubin, L. L., and Porter, J. A. (2002) Small-molecule modulators of Hedgehog signaling: identification and characterization of Smoothed agonists and antagonists. *J. Biol.* 1, 10.
- (2) Heal, W. P., Jovanovic, B., Bessin, S., Wright, M. H., Magee, A. I., and Tate, E. W. (2011) Bioorthogonal chemical tagging of protein cholesterylation in living cells. *Chem. Commun. Camb. Engl.* 47, 4081–4083.
- (3) Broncel, M., Serwa, R. A., Ciepla, P., Krause, E., Dallman, M. J., Magee, A. I., and Tate, E. W. (2015) Multifunctional reagents for quantitative proteome-wide analysis of protein modification in human cells and dynamic profiling of protein lipidation during vertebrate development. *Angew. Chem. Int. Ed Engl.* 54, 5948–5951.
- (4) Lanyon-Hogg, T., Ritzefeld, M., Masumoto, N., Magee, A. I., Rzepa, H. S., and Tate, E. W. (2015) Modulation of Amide Bond Rotamers in 5-Acyl-6,7-dihydrothieno[3,2-c]pyridines. *J. Org. Chem.* 80, 4370–4377.
- (5) Lanyon-Hogg, T., Masumoto, N., Bodakh, G., Konitsiotis, A. D., Thinon, E., Rodgers, U. R., Owens, R. J., Magee, A. I., and Tate, E. W. (2015) Click chemistry armed enzyme-linked immunosorbent assay to measure palmitoylation by hedgehog acyltransferase. *Anal. Biochem.* 490, 66–72.
- (6) Lanyon-Hogg, T., Masumoto, N., Bodakh, G., Konitsiotis, A. D., Thinon, E., Rodgers, U. R., Owens, R. J., Magee, A. I., and Tate, E. W. (2016) Synthesis and characterisation of 5-acyl-6,7-dihydrothieno[3,2-c]pyridine inhibitors of Hedgehog acyltransferase. *Data Brief* 7, 257–281.
- (7) Liu, J., Pan, S., Hsieh, M. H., Ng, N., Sun, F., Wang, T., Kasibhatla, S., Schuller, A. G., Li, A. G., Cheng, D., Li, J., Tompkins, C., Pferdekamper, A., Steffy, A., Cheng, J., Kowal, C., Phung, V., Guo, G., Wang, Y., Graham, M. P., Flynn, S., Brenner, J. C., Li, C., Villarreal, M. C., Schultz, P. G., Wu, X., McNamara, P., Sellers, W. R., Petruzzelli, L., Boral, A. L., Seidel, H. M., McLaughlin, M. E., Che, J., Carey, T. E., Vanasse, G., and Harris, J. L. (2013) Targeting Wnt-driven cancer through the inhibition of Porcupine by LGK974. *Proc. Natl. Acad. Sci.* 110, 20224–20229.
- (8) Konitsiotis, A. D., Chang, S.-C., Jovanović, B., Ciepla, P., Masumoto, N., Palmer, C. P., Tate, E. W., Couchman, J. R., and Magee, A. I. (2014) Attenuation of hedgehog acyltransferase-catalyzed sonic Hedgehog palmitoylation causes reduced signaling, proliferation and invasiveness of human carcinoma cells. *PLoS One* 9, e89899.
- (9) Taipale, J., Chen, J. K., Cooper, M. K., Wang, B., Mann, R. K., Milenkovic, L., Scott, M. P., and Beachy, P. A. (2000) Effects of oncogenic mutations in Smoothed and Patched can be reversed by cyclopamine. *Nature* 406, 1005–1009.
- (10) Chen, B., Dodge, M. E., Tang, W., Lu, J., Ma, Z., Fan, C.-W., Wei, S., Hao, W., Kilgore, J., Williams, N. S., Roth, M. G., Amatruda, J. F., Chen, C., and Lum, L. (2009) Small molecule-mediated disruption of Wnt-dependent signaling in tissue regeneration and cancer. *Nat. Chem. Biol.* 5, 100–107.

(11) Ciepla, P., Konitsiotis, A. D., Serwa, R. A., Masumoto, N., Leong, W. P., Dallman, M. J., Magee, A. I., and Tate, E. W. (2014) New chemical probes targeting cholesterylation of Sonic Hedgehog in human cells and zebrafish. *Chem. Sci. R. Soc. Chem.* 2010 5, 4249–4259.

(12) Rappsilber, J., Mann, M., and Ishihama, Y. (2007) Protocol for micro-purification, enrichment, pre-fractionation and storage of peptides for proteomics using StageTips. *Nat. Protoc.* 2, 1896–1906.

(13) Wilson, J. P., Raghavan, A. S., Yang, Y.-Y., Charron, G., and Hang, H. C. (2011) Proteomic analysis of fatty-acylated proteins in mammalian cells with chemical reporters reveals S-acylation of histone H3 variants. *Mol. Cell. Proteomics MCP* 10, M110.001198.

(14) Davidson, R. K., Waters, J. G., Kevorkian, L., Darrah, C., Cooper, A., Donell, S. T., and Clark, I. M. (2006) Expression profiling of metalloproteinases and their inhibitors in synovium and cartilage. *Arthritis Res. Ther.* 8, R124.